SUPPLEMENTARY DATA

Angiogenic Factor AGGF1-Primed Endothelial Progenitor Cells Repair Vascular Defect in Diabetic Mice

Yufeng Yao, Yong Li, Qixue Song, Changqin Hu, Wen Xie, Chengqi Xu, Qiuyun Chen, and Qing K. Wang

SUPPLEMENTARY DATA

Supplementary Figure S1. Isolation and characterization of bone marrow derived EPCs from mice. Bone marrow mononuclear cells (MNCs) were washed out from the femurs and tibias of mice and isolated by density gradient centrifugation with histopaque-1083. MNCs were plated on gelatin-coated culture dishes and maintained in endothelial growth factor–supplemented media (EGM-2 bullet kit. Ten days after maintenance in endothelial-specific media, non-adherent MNCs were removed and the remaining adherent cells were subjected to immunostaining to verify their EPC identity. (**A)** Morphology of MNCs on day 4 and day 8 after plating on gelatin-coated dishes. Scale bar=50 μm. (**B)** Representative images from assays for uptake of Dil-acLDL (red fluorescence) and FITC-UEA-1 (green fluorescence). The isolated EPCs were Dil-acLDL and FITC-UEA-1 positive. Blue, staining of the nuclei by Hoechst. Scale bar=50 μm（upper）, Scale bar=100 μm（lower）. Three independent experiments were performed. (**C)** MNCs were cultured in the bullet kit medium in gelatin-coated cell culture dishes. Ten days after plating, adherent cells were further analyzed using flow cytometry with the cell surface antigen markers, including antibodies for CD31, CD34, CD45 and CD144. Isotype IgG was used as a control antibody. Six mice per group (n=6/group) were studied each time.

SUPPLEMENTARY DATA

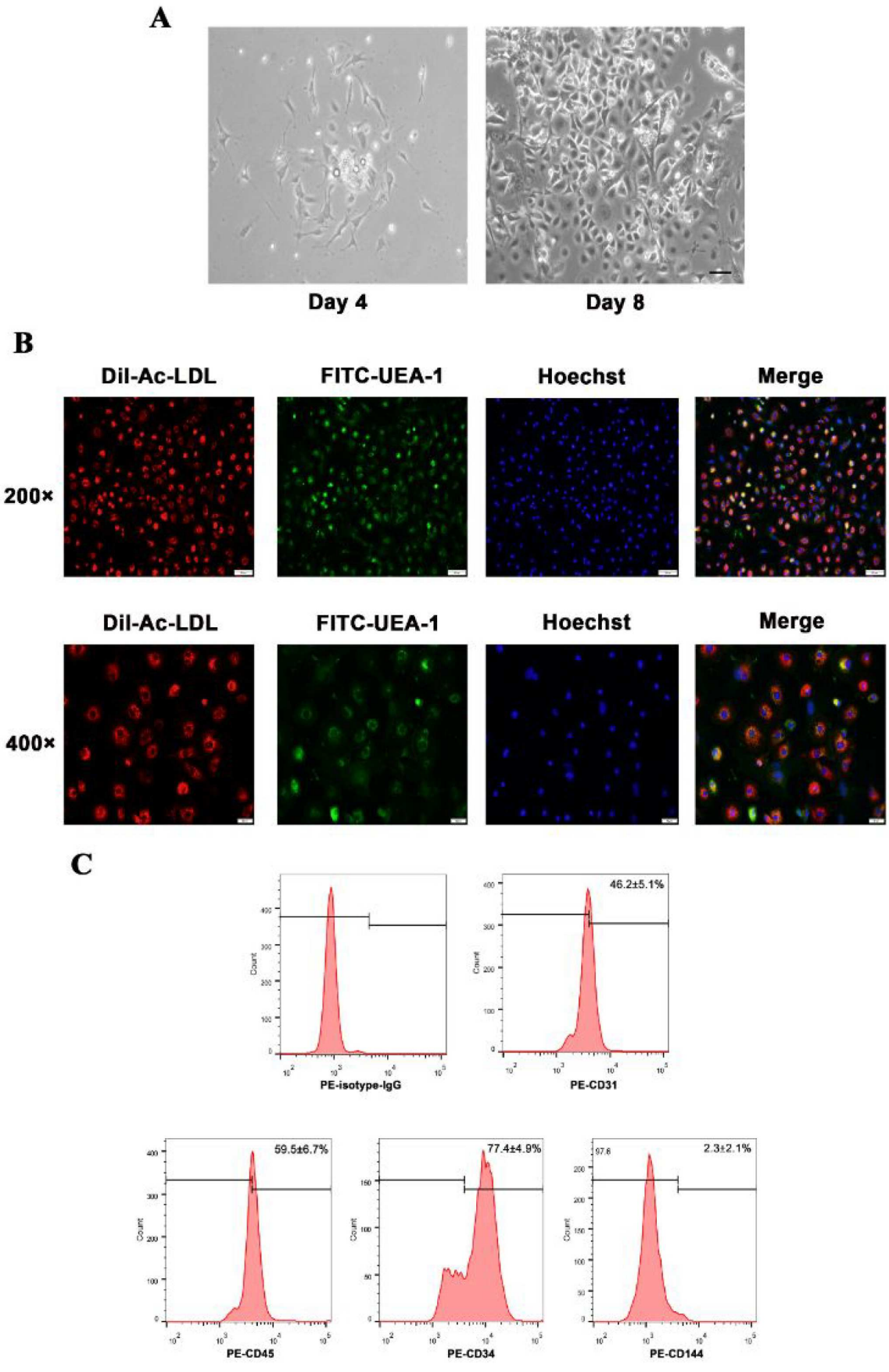

SUPPLEMENTARY DATA

SUPPLEMENTARY DATA

Supplementary Figure S2. *Aggf1* haploinsufficiency significantly reduces the number of bone marrow mononuclear cells (MNCs). MNCs were washed out from the femurs and tibias of WT and *Aggf1*$^{+/-}$ KO mice and purified by density gradient centrifugation with histopaque-1083. MNCs were plated into gelatin-coated culture dishes and maintained in endothelial growth factor–supplemented media (EGM-2 bullet kit for ten days. Non-adherent MNCs were removed and the remaining adherent cells were subjected to immunostaining to verify their EPC identity. (**A)** Representative images from assays for uptake of Dil-Ac-LDL (red fluorescence) and FITC-UEA-1 (green fluorescence) are shown in (**A**). The isolated EPCs were Dil-ALDL- and FITC-UEA-1 positive. Blue, staining of the nuclei by Hoechst. **(B)** The number of the Dil-acLDL/FITC-UEA-1 (lectin) positive cells was plotted and compared between WT and *Aggf1*$^{+/-}$ KO mice. Scale bar=100 μm. Three independent experiments were performed. Six mice per group (n=6/group) were studied each time. Data are shown as mean ± SD. **P*<0.05.

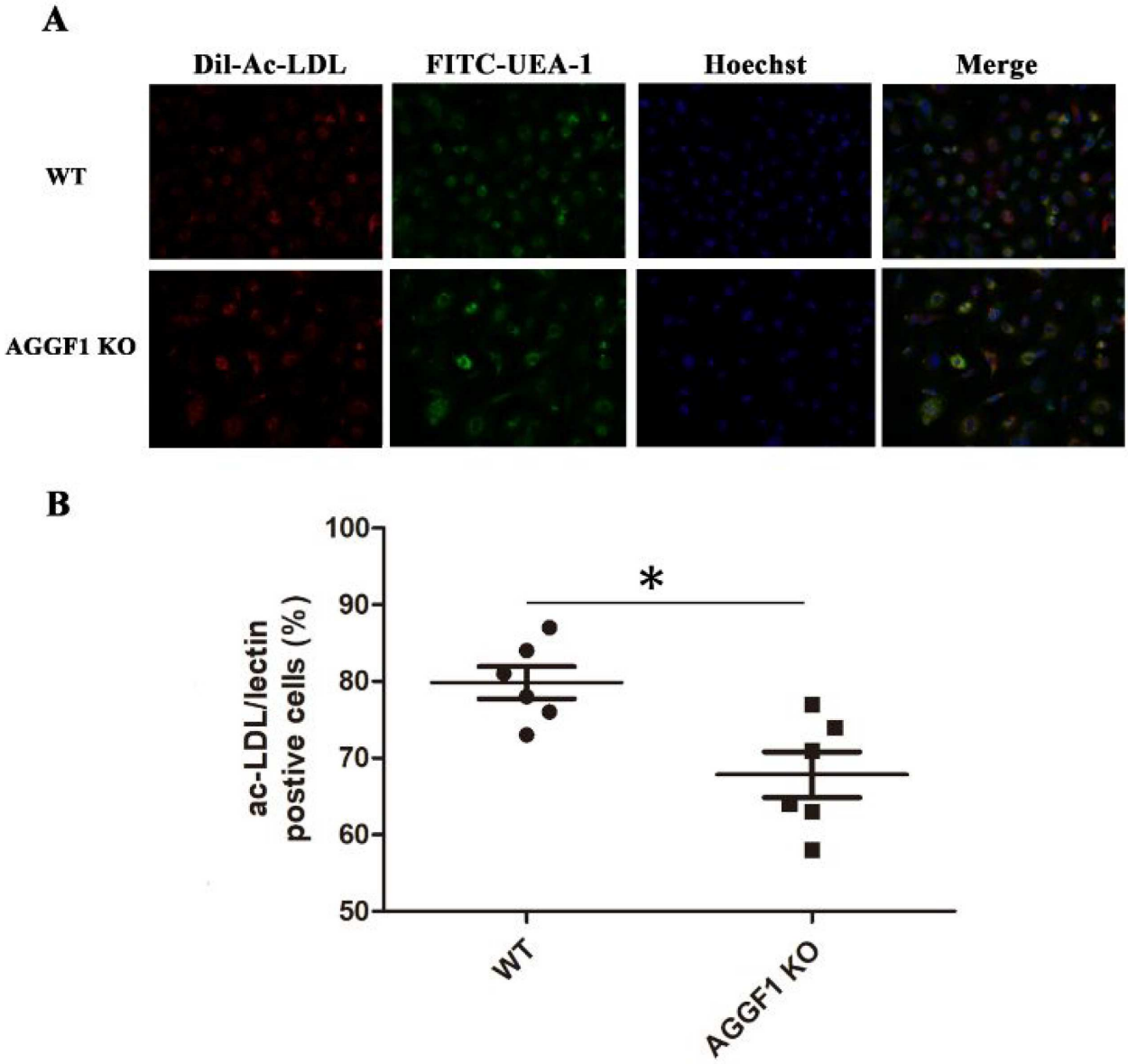

SUPPLEMENTARY DATA

Supplementary Figure S3. The expression level of the AGGF1 protein is increased in EPCs isolated from *db/db* mice or mice treated with HFD. **(A)** Western blot analysis showing increased AGGF1 expression in isolated EPCs from *db/db* mice. **(B)** Western blot analysis showing increased AGGF1 expression in isolated EPCs from HFD-induced T2DM mice. GAPDH was used as loading control. Data are shown as mean ± SD. ***P*<0.01, (n=6).

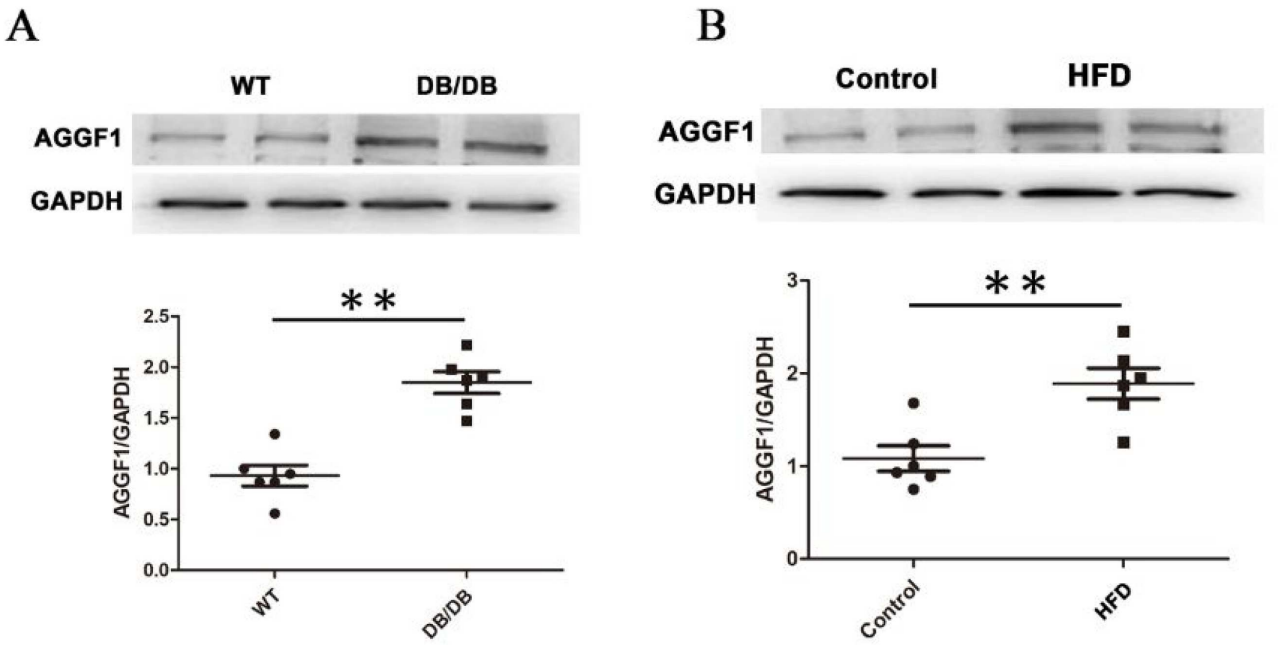

SUPPLEMENTARY DATA

Supplementary Figure S4. Increased glucose levels in mice fed with a high fat diet (HFD). C57BL/6J mice were fed with a high fat diet **alone** to induce T2DM. Mice fed with a chow diet were sued as controls. After 16 weeks, blood glucose levels were measured using a glucometer, and then a hind-limb ischemia model was established with the mice. Three independent experiments were performed. Data are shown as mean ± S.D. ***P*<0.01 (n=6).

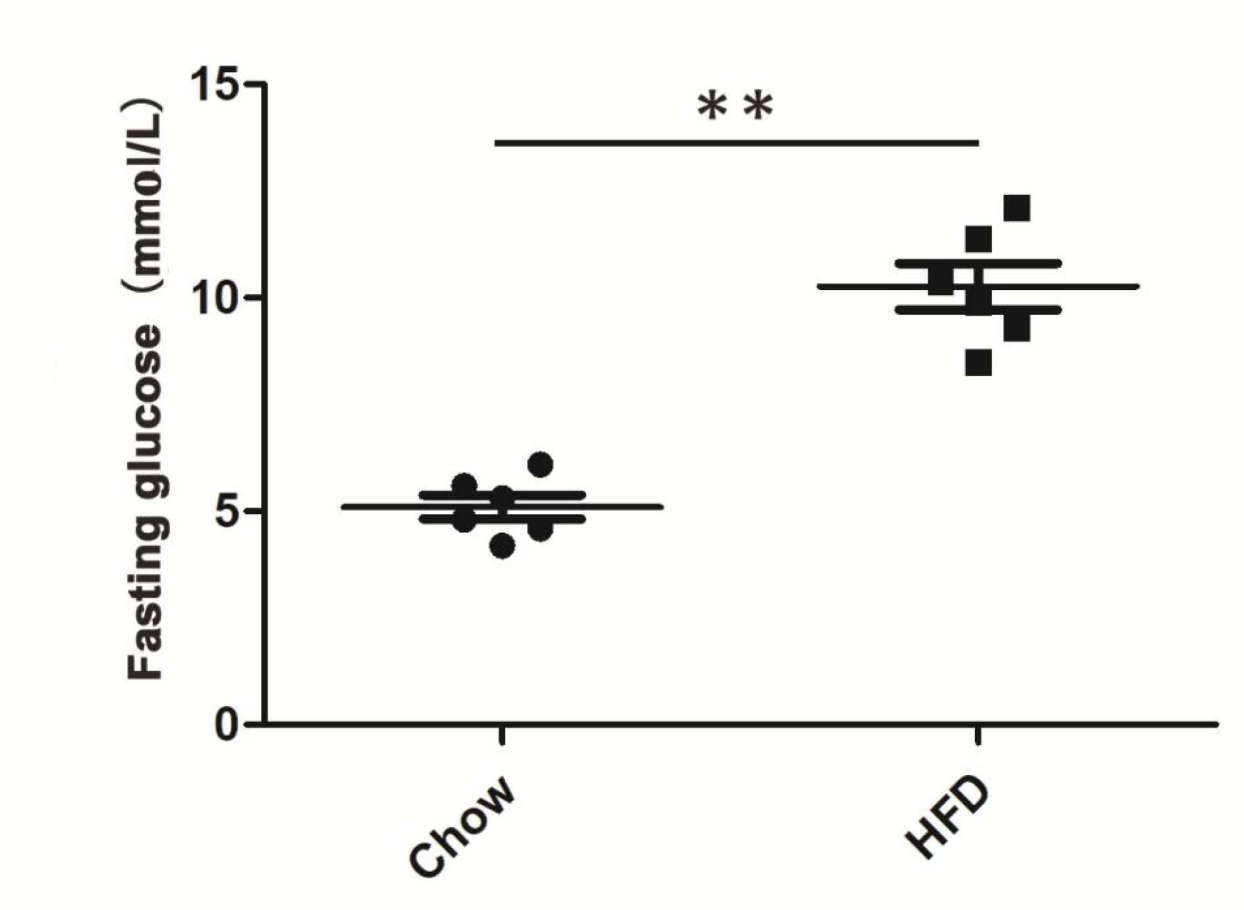

SUPPLEMENTARY DATA

Supplementary Figure S5. Analysis of the expression levels of *CXCR4*, *VEGF* and *VEGFR2* mRNA in EPCs from different groups of mice. Bone marrow-derived EPCs were isolated and used for real-time RT-PCR analysis. Data are shown as mean ± SD. NS not significant, (n=3).

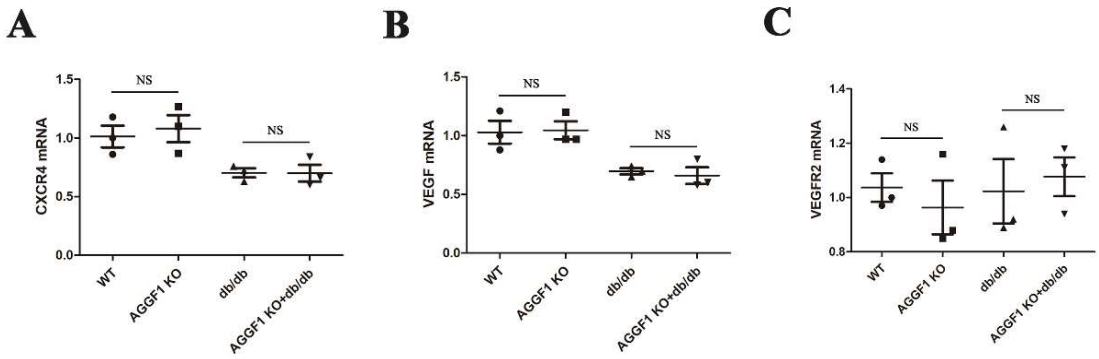

SUPPLEMENTARY DATA

Supplementary Figure S6. *Aggf1* is required for essential functions of EPCs in capillary tube formation, proliferation, transendothelial migration, and migration as in a HFD-induced diabetic mouse model. EPCs were isolated from bone marrow of wild-type (WT) and heterozygous *Aggf1*$^{+/-}$ knockout (KO) mice fed with and without a high glucose diet (HFD), and characterized. (**A)** *Aggf1* haploinsufficiency inhibits angiogensis mediated by EPCs. Angiogenic function of EPCs was assessed by a matrigel-based capillary tube formation. (**B)** Images from **(A)** were analyzed, quantified and plotted. **(C)** *Aggf1* haploinsufficiency inhibits EPC proliferation. Proliferation of EPCs was examined using the CCK-8 kit. (**D)** *Aggf1* haploinsufficiency inhibits transendothelial migration of EPCs in transwell assays. HUVECs (about 1×10^4 cells per well) were cultured in the upper chamber of a 24-transwell insert (8.0-μm pores). EPCs were harvested, resuspended in basal culture medium (EBM-2, 0.5% BSA), and added to the upper chamber of the transwell plate (0.2 ml). Images were captured 24 hours after EPCs plating with an inverted Nikon Eclipse Ti microscope. (**E)** Images from (**D)** were quantified and plotted. (**F)** *Aggf1* haploinsufficiency inhibits EPC migration in wound scratch migration assays. EPCs monolayers in 6-well cell culture plates were wounded with a scratch by a 200 μl pipette tip and examined 24 hours after wounding. Images were captured with an inverted Nikon Eclipse Ti microscope. (**G)** Representative images from EPC migration assays. Data are shown as mean ± SD. **P*<0.05, ***P*<0.01, ****P*<0.001 (n=6 mice per group).

SUPPLEMENTARY DATA

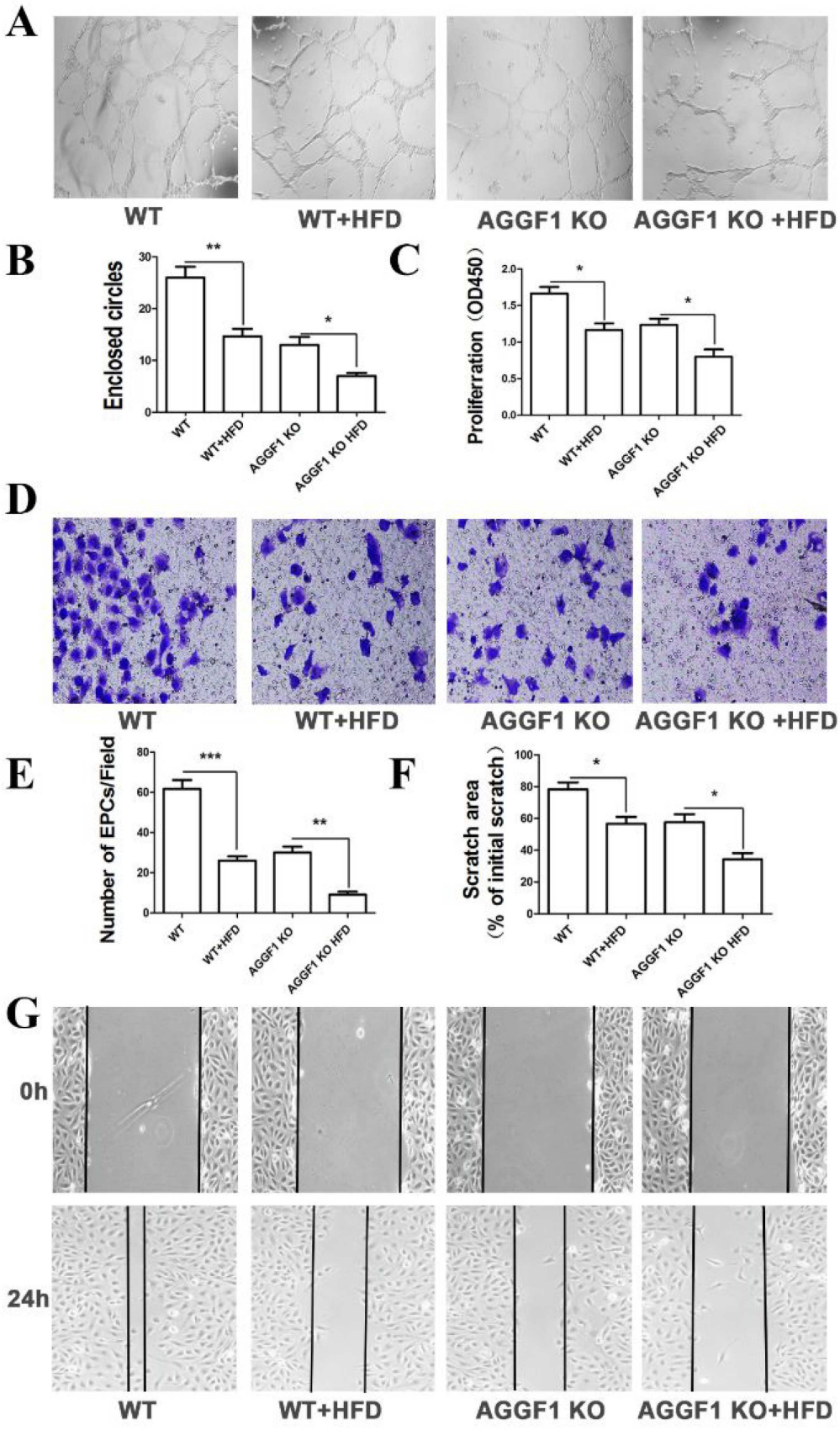

SUPPLEMENTARY DATA

Supplementary Figure S7. Analysis of the expression levels of *CXCR4, VEGF* and *VEGFR2* mRNA in EPCs from mice treated with the AGGF1 protein and high glucose. EPCs were isolated, and used for real-time RT-PCR analysis. Data are shown as mean ± SD. NS not significant, (n=3).

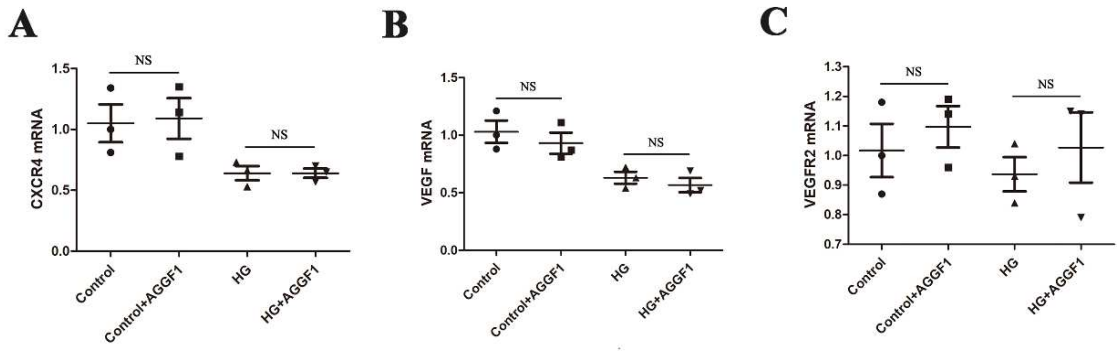

SUPPLEMENTARY DATA

Supplementary Figure S8. AGGF1 protein treatment robustly potentiates the therapeutic effects of EPCs on angiogenesis and homing in a hindlimb ischemia model in *db/db* mice. (A) Representative images for H&E staining and immunostaining for CD31. Scale bar=100 μm. **(B)** Representative images for immunostaining with an anti-GFP antibody. EPCs were infected with EGFP lentivirus, and transplanted into *db/db* mice with diabetic hind-limb ischemia. Scale bar=200 μm. (n=12 mice per group).

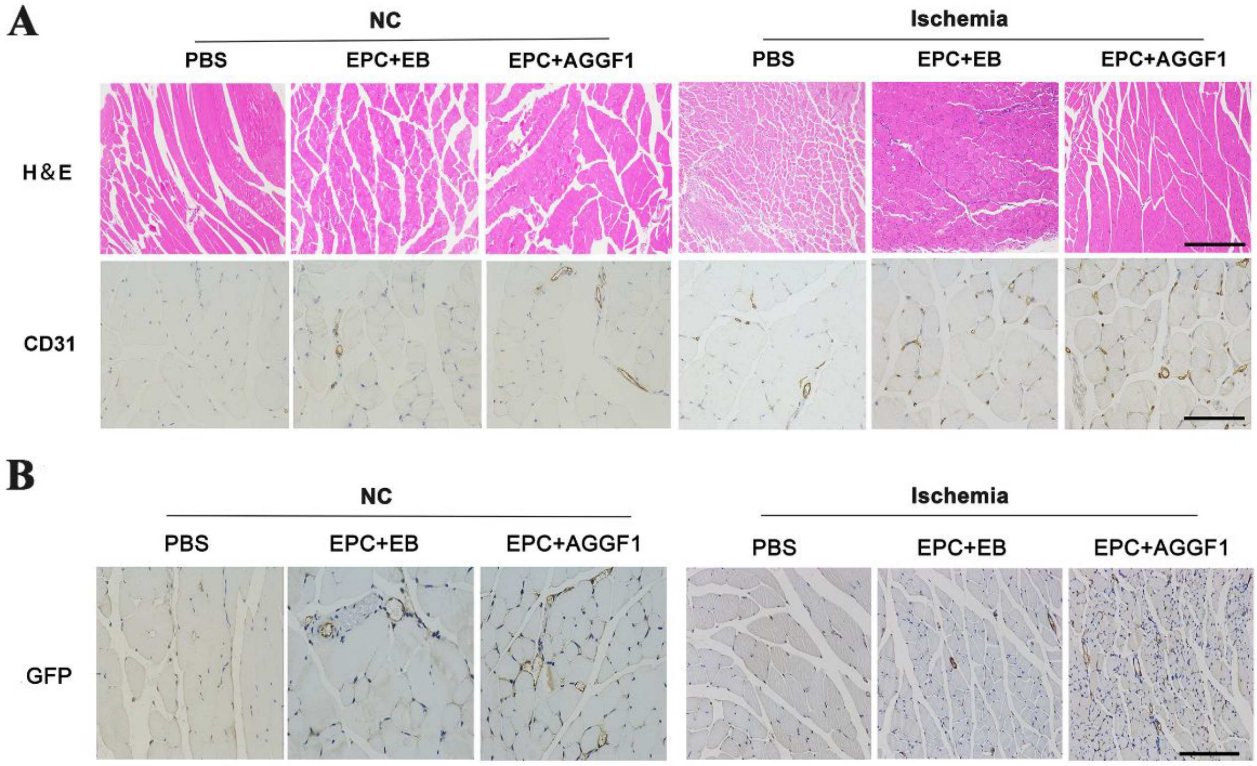

SUPPLEMENTARY DATA

Supplementary Figure S9. AGGF1 protein treatment robustly potentiates the therapeutic effects of EPCs on peripheral vascular complications in a hindlimb ischemia model. A hindlimb ischemia model was created in mice. Two days after the surgery, the mice were injected with EPCs, AGGF1-pretrearted EPCs (~1×10^6), and control PBS via the tail vein. The therapeutic effects were evaluated using a Vevo 2100 High-Resolution Micro-Ultrasound System before the ischemic surgery and 7, 14 and 28 days after ischemia. (**A)** Transplantation of AGGF1-pretreated EPCs dramatically improved blood perfusion compared with EPCs without AGGF1 pretreatment. (**B)** Therapeutic effects of AGGF1-pretreated EPCs on necrosis compared with EPCs without AGGF1 pretreatment. **(C)** Therapeutic effects of AGGF1-pretreated EPCs on ambulatory impairment compared with EPCs without AGGF1 pretreatment. (**D)** Effects of AGGF1-pretreated EPCs on the density of CD31-postive capillary vessels compared with EPCs without AGGF1 pretreatment. Capillary density was measured in HFD-fed HLI mice. The gastrocnemius muscle from HLI mice were fixed in 4% paraformaldehyde for 24 hours and used for immunostaining analysis with an anti-CD31 antibody. (**E)** Representative images for H&E staining and immunostaining for CD31. Scale bar=100 μm. (**F)** Representative images for immunostaining with an anti-GFP antibody. EPCs were infected with EGFP lentivirus, and transplanted into mice with diabetic hind-limb ischemia. Four weeks after transplantation, the gastrocnemius muscle were fixed in 4% paraformaldehyde for 24 hours and then subjected to immunostaining analysis with an anti-EGFP antibody to determine whether EPCs were homed into the ischemic areas. Scale bar=100 μm. Data are shown as mean ± SD. **P*<0.05, ***P*<0.01 (n=12 mice per group).

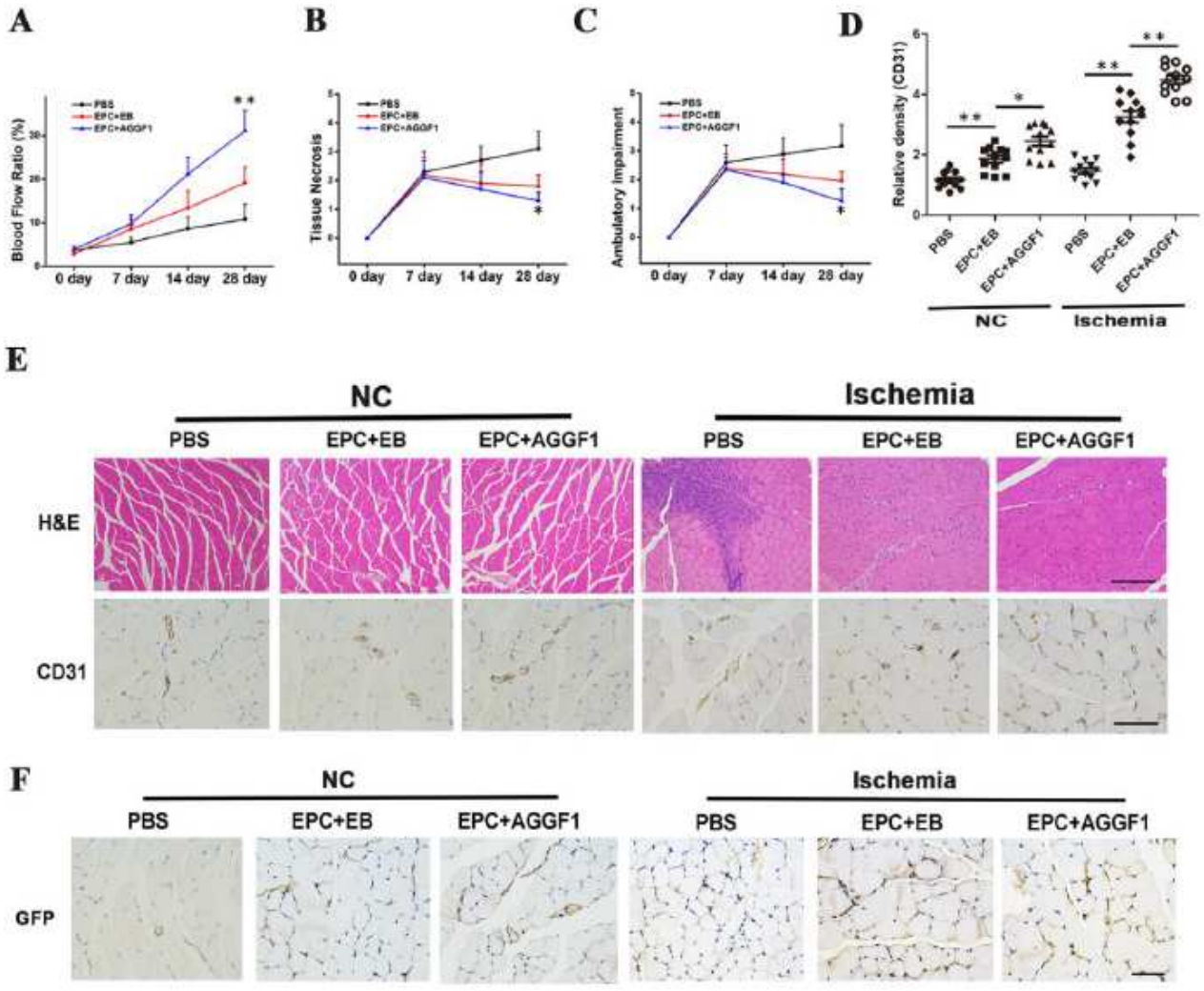

SUPPLEMENTARY DATA

Supplementary Figure S10. EPCs were infected lentiviruses with GFP expression as an easily identifiedable marker. The infection efficiency and the level of GFP expression were evaluated 72 h after infection. Scale bar=20 μm. Three independent experiments were performed and representative images were shown. Images were captured at the magnification of 40×.

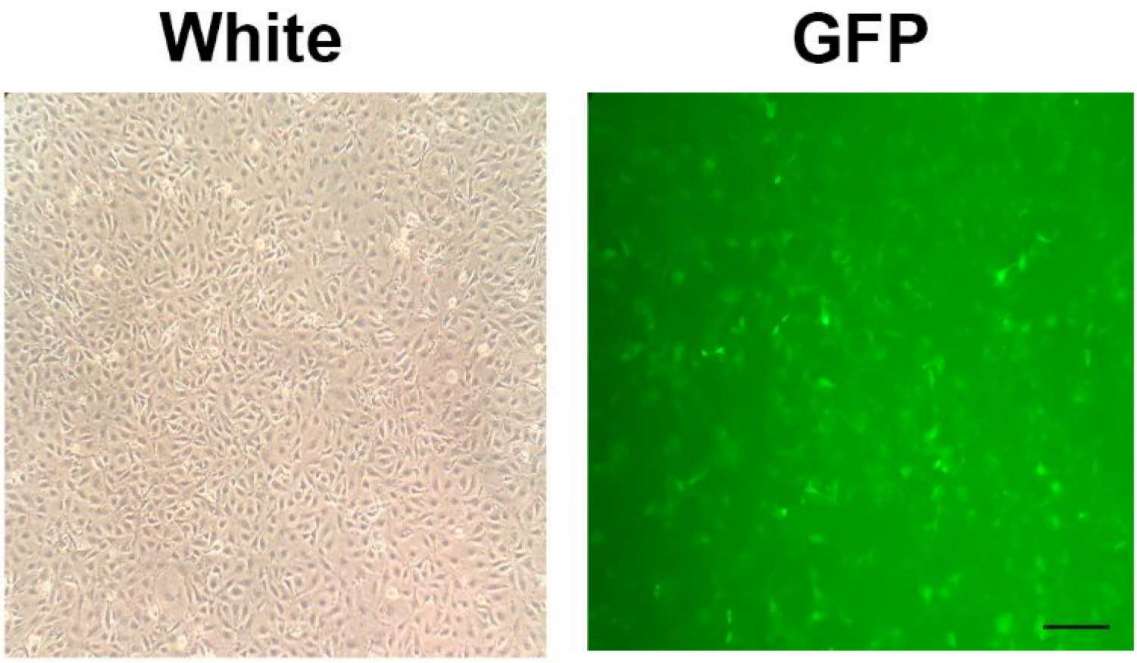

SUPPLEMENTARY DATA

Supplementary Figure S11. AGGF1 inhibits HG-induced superoxide production by EPCs. Dichlorodihydrofluorescein diacetate (DCFH-DA, sigma) was used to detect superoxide in EPCs with flow cytometry (Beckman CytoFLEX). Fluorescence intensity was recorded, analyzed and plotted. Data are shown as mean ± SD. *P<0.05, **P<0.01, (n=6 per group).

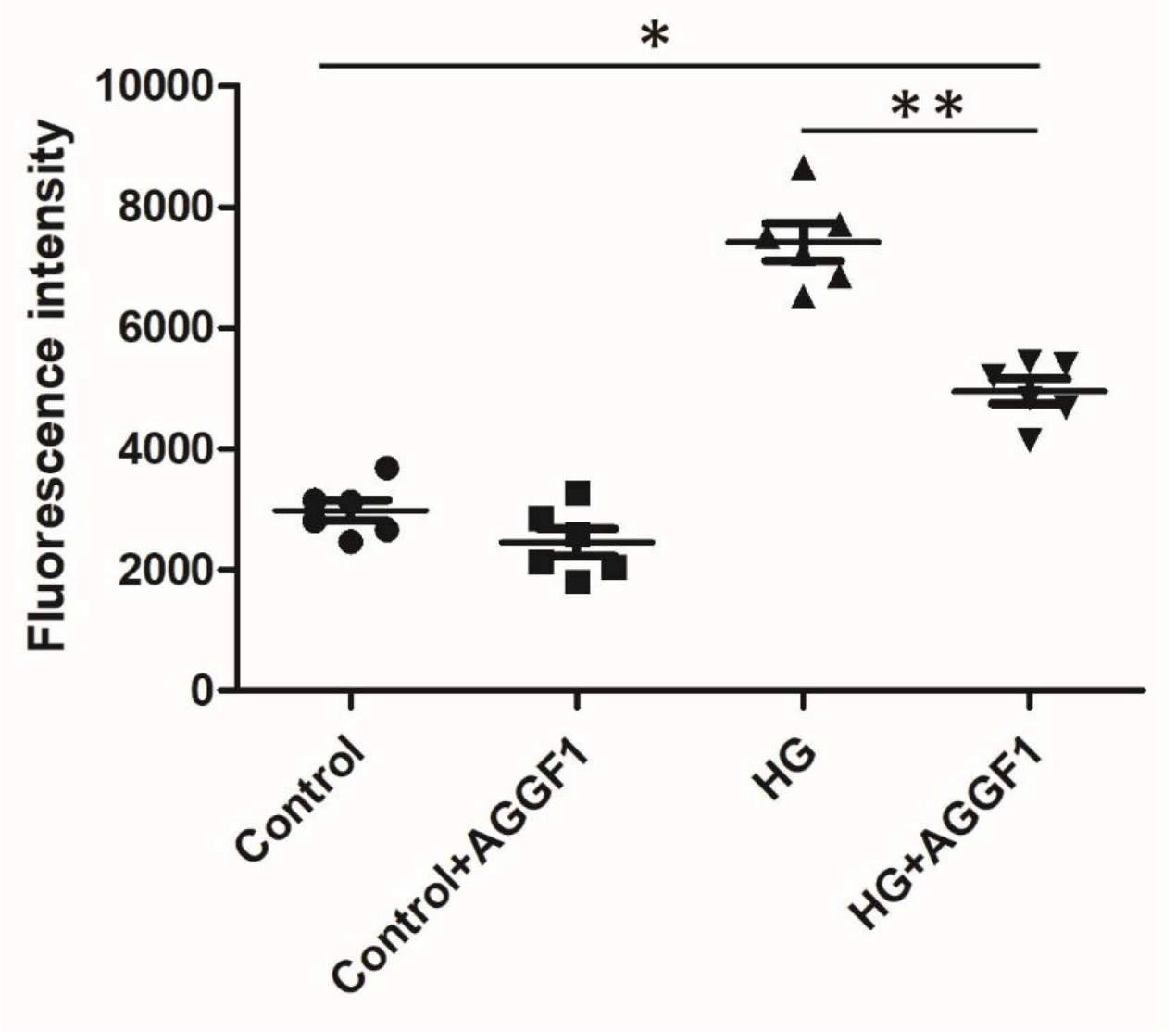

SUPPLEMENTARY DATA

Supplementary Figure S12. AGGF1 increases the level of nuclear Nrf2 in EPCs. EPCs were treated with a high glucose solution (HG) in the presence or absence of purified AGGF1 protein for 12 hours, and used for immunofluorescent staining with an anti-Nrf2 antibody to analyze nuclear translocation of Nrf2. Scale bar=200 μm.

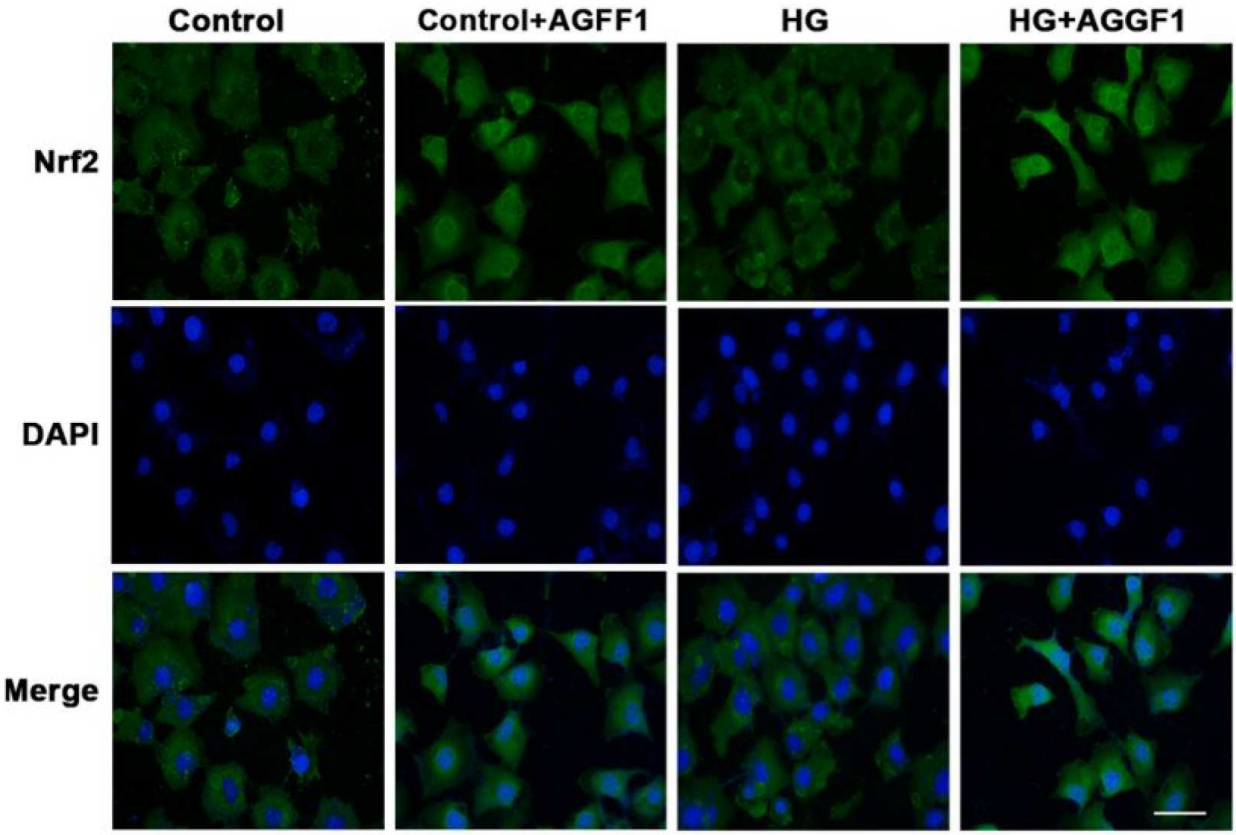

SUPPLEMENTARY DATA

Supplementary Figure S13. AGGF1 does not affect the expression levels of Nrf2 and KEAP-1 in EPCs. EPCs were cultured in media with or without high glucose (HG, 30 mM) as well as a combination of high glucose and AGGF1 protein. (**A**) Total RNA was extracted with Trizol reagent and used for real-time RT-PCR analysis for the level of *Nrf2* mRNA. (**B**) Western blot analysis with an anti-Nrf2 antibody. (**C**) Western blot analysis using an anti-KEAP-1 antibody. GAPDH was used as loading control. Three independent experiments were performed. Data are shown as mean ± S.D, (n=6).

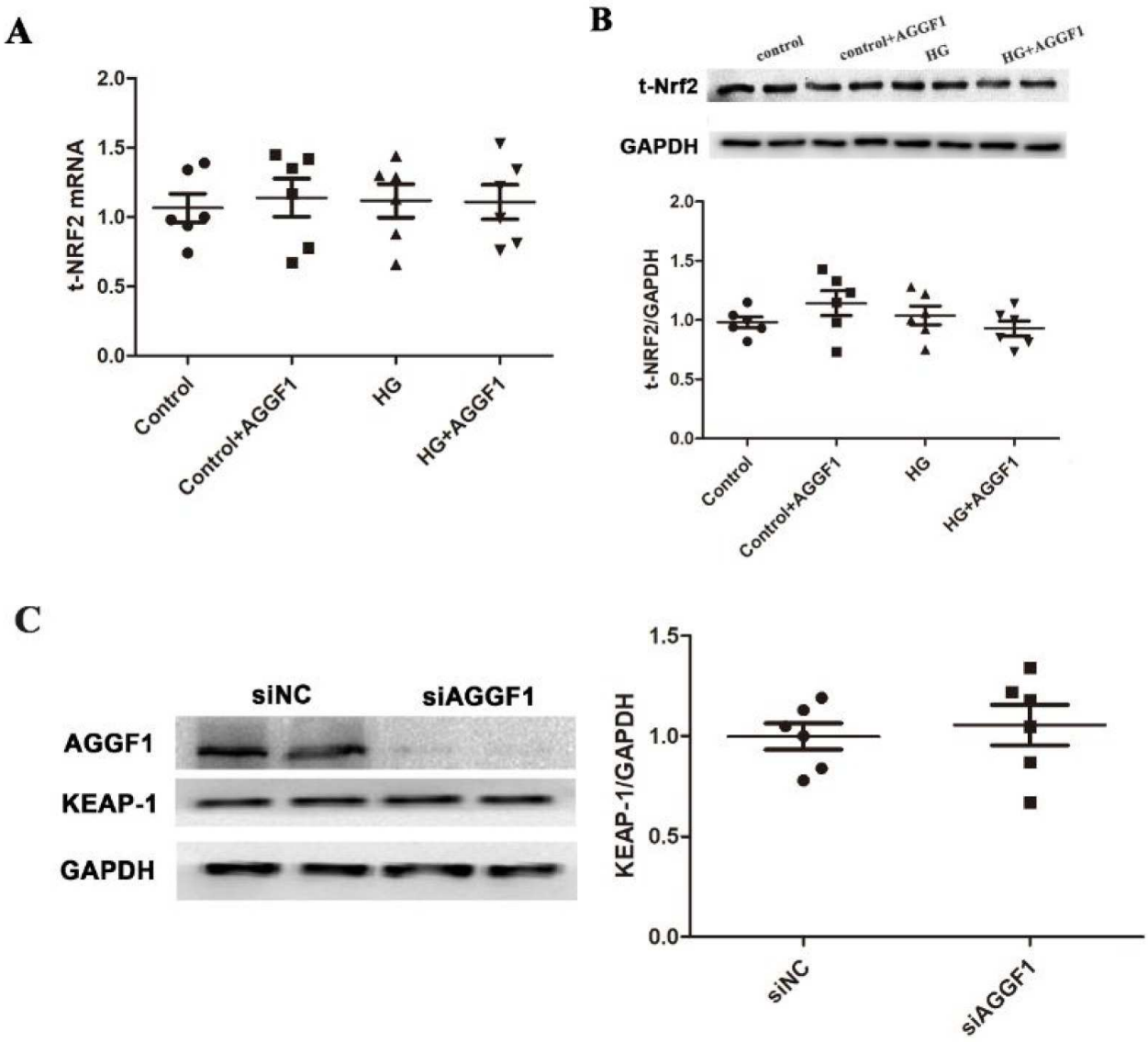

SUPPLEMENTARY DATA

Supplementary Figure S14. Western blot analysis for nuclear **accumulation of nNrf2 in EPCs treated with *Aggf1* siRNA and *Fyn* siRNA under the normal condition (Control) and under a high glucose condition (HG).** GAPDH was used as loading control.

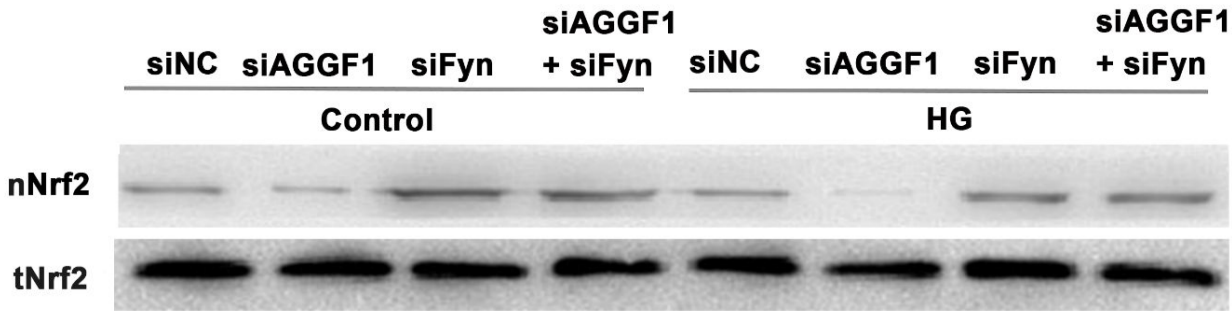

SUPPLEMENTARY DATA

Supplementary Figure S15. A schematic diagram showing the molecular signaling pathway by which AGGF1 protein therapy potentiates the therapeutic effects of EPCs on diabetes-induced vascular complications. AGGF1 activates AKT signaling, which inhibits Fyn-mediated export and degradation of nuclear Nrf2. Nrf2 binds to the promoter and regulatory region and activate the transcription of *CAT*, HQ-1, and *NQO-1*, which function as antioxidants to block generation of ROS, reducing oxidative stress and increasing function of EPCs. Overall, AGGF1 functions as an antioxidant regulator to protect the function of EPCs, and becomes a potential therapeutic target for improving the ischemia-reparative capacity of EPCs transplantation in DM.